On the Kinetics of Ionic Liquid Adsorption onto Activated Carbons from Aqueous Solution

ARTICLE *in* INDUSTRIAL & ENGINEERING CHEMISTRY RESEARCH · JANUARY 2013

Impact Factor: 2.59 · DOI: 10.1021/ie3028729

4 AUTHORS, INCLUDING:

Jesus Lemus
University of Aveiro
16 PUBLICATIONS **473** CITATIONS

SEE PROFILE

I&EC research
Industrial & Engineering Chemistry Research

Article

pubs.acs.org/IECR

On the Kinetics of Ionic Liquid Adsorption onto Activated Carbons from Aqueous Solution

Jesús Lemus,* Jose Palomar, Miguel A. Gilarranz, and Juan J. Rodriguez

Sección de Ingeniería Química, Departamento de Química Física Aplicada, Universidad Autónoma de Madrid, Cantoblanco, 28049 Madrid, Spain

Supporting Information

ABSTRACT: Adsorption with activated carbons (ACs) has been recently proposed as a thermodynamically favored treatment to remove and/or recover ionic liquids (ILs) from aqueous streams. In this work, a kinetic analysis of the adsorption of a hydrophobic IL (1-methyl-3-octylimidazolium hexafluorophosphate, $OmimPF_6$) by commercial ACs was performed. The results indicated that adsorption kinetics is remarkably slower for the IL than for phenol, used as a reference solute. Then, the effects of the main operating conditions (stirring, AC particle size, temperature, and initial concentration of IL) on the adsorption rate were investigated. For the purpose of developing criteria to improve the kinetics of IL adsorption with ACs, different empirical and phenomenological kinetic models were applied to describe the experimental adsorption data. The kinetic analysis indicated that the mechanism of IL adsorption onto ACs is mainly controlled by the mass transfer into the pores. Therefore, the selection of adequate particle size of the adsorbent plays a major role in the development of feasible IL adsorption. Increasing the temperature led to significantly faster adsorption, which was found to be of interest for removing and/or recovering IL from aqueous solution in spite of the associated decrease of equilibrium capacity.

1. INTRODUCTION

During the past decade, ionic liquids (ILs) have become one of the most promising and rapidly developing areas of modern chemistry, technology, and engineering, focusing on the ultimate aim of large scale industrial applications.[1,2] ILs are characterized by their exceptional properties such as negligible vapor pressure and nonflammability under ambient conditions, high thermal and chemical stability, wide liquid window and high solvent capacity.[3−5] However, probably the most important attribute of ILs is the possibility of designing their properties by an adequate selection of the counterions. Thanks to the enormous number of cation and anion combinations, ILs can possess a wide spectrum of physical and chemical properties (solubility, polarity, viscosity, etc.), and they are already recognized by the chemical industry as new target-oriented reaction and separation media.[6,7] However, the application of ILs on the industrial scale may involve an environmental risk as a result of their transport, storage, release in wastewaters, etc.[8,9] Therefore, the removal/recovery of ILs from aqueous streams has to be taken into account for a proper use of ILs in industrial processes, since it has been recently demonstrated that ILs present a wide range of toxicity and biodegradability.[10−12]

Destructive and nondestructive treatments for the removal of ILs from aqueous effluents have been recently investigated. The most studied destructive techniques include advanced oxidation[13,14] and biological treatments.[15,16] It is important to consider that ILs are still quite expensive, and their recycling after regeneration or recovery needs to be regarded.[8] Among available nondestructive technologies, distillation,[17] crystallization,[18] nanofiltration,[19] pervaporation,[20,21] and adsorption onto solids[21−26] are being increasingly studied. Adsorption by activated carbons (ACs) has been recently demonstrated as an effective nondestructive technique for removing ILs from aqueous solutions and recovering them for the process.[23,24] ACs are interesting candidates among other adsorbents[27] due to their high surface area, surface chemistry tailoring, harmfulness to the environment, and easy handling in operation.[28] Previous adsorption equilibrium analysis by our group[23,24] showed that the structural properties and chemical surface of the AC can be conveniently modified to adsorb efficiently ILs with different structures, indicating the viability of IL adsorption from a thermodynamic point of view. However, the kinetic aspects have been not discussed in our previous works, and it is necessary to know them for design purposes. Several empirical and phenomenological kinetic models have been applied to describe the adsorption rate of organic solutes onto different adsorbents,[29−31] as they can provide insight in the adsorption mechanisms for further design of adsorption systems. A recent study by Duclaux et al.,[25] focused on the adsorption of hydrophilic ILs by ACs, showed that not only thermodynamics but also kinetics of ILs adsorption were dependent on the properties of the AC adsorbent, suggesting the need of checking different kinetic models according to the ACs used.[25]

In this work, a detailed kinetic analysis of the adsorption of a hydrophobic IL (1-octyl-3-methylimidazolium hexafluorophosphate, $OmimPF_6$) from water onto different commercial ACs has been performed from the adsorption kinetic curves obtained in batch stirred tank at different operating conditions. First, the kinetics of IL ($OmimPF_6$) adsorption was compared

Received: October 20, 2012
Revised: January 27, 2013
Accepted: January 28, 2013
Published: January 28, 2013

   dx.doi.org/10.1021/ie3028729 | Ind. Eng. Chem. Res. 2013, 52, 2969−2976

Table 1. Characterization of the Fresh and Modified ACs

	A_{BET} ($m^2 \cdot g^{-1}$)	A_S ($m^2 \cdot g^{-1}$)	$V_{microp.}$ ($cm^3 \cdot g^{-1}$)	$V_{mesop.}$ ($cm^3 \cdot g^{-1}$)	groups evolved as CO_2 ($\mu mol \cdot g^{-1}$)	groups evolved as CO ($\mu mol \cdot g^{-1}$)
MkU	927	155	0.36	0.14	183	490
MkU-900	906	102	0.32	0.09	113	323
ENA	912	350	0.4	0.4	108	116
ENA-900	901	339	0.34	0.4	73	99
CAP	1915	667	0.66	0.63	1204	1863
CAP-900	1434	346	0.51	0.42	228	247

to that of a reference organic solute (phenol). Second, a systematic screening of different kinetic models, developed for organic solutes, was performed to better describe the IL adsorption rate onto AC. Those models included pseudo-first-order, second order, Lagergren, and intraparticle diffusion.[32−34] The operating variables, whose influence in the adsorption kinetics and thermodynamics of $OmimPF_6$ onto commercial ACs was evaluated, were stirring velocity (200−700 rpm), AC particle size (100−2000 μm), initial concentration of $OmimPF_6$ (0.1−3.2 $mmol \cdot L^{-1}$), and temperature (308−348 K). Summarizing, the kinetic analysis performed provides insights on the optimization of the operating conditions for the adsorption of ILs by ACs, useful for the design of viable systems for the removal and recovery of ILs from industrial aqueous streams.

2. MATERIALS AND METHOD

2.1. Materials and Characterization Methods. Three commercial ACs were tested in this study, supplied by Merck (1.02514.100, MkU), Norit (CAP SUPER), and Timcal (Enasco 350G). The ACs were sieved to different ranges of particle size (d_p: 2000−1000 μm; 1000−500 μm; 500−300 μm; 300−100 μm; and <100 μm). The commercial ACs were subjected to a thermal treatment in order to reduce the surface oxygen groups concentration, thus reducing their differences in surface chemical composition. The thermal treatment of the ACs was accomplished in a quartz horizontal tube furnace (2.5 cm inner diameter (i.d.) and 15 cm length) under a nitrogen flow of 60 $mL \cdot min^{-1}$ at 1173 K. This temperature was reached at a 100 $K \cdot min^{-1}$ rate and maintained for 3 h.

The porous structure of the adsorbents was characterized by means of 77 K N_2 adsorption−desorption using a Micromeritics apparatus (Tristar II 3020 model). Previous to N_2 adsorption, the samples were outgassed at 423 K for 8 h under a constant flow of N_2 at atmospheric pressure. The Brunauer−Emmett−Teller (BET) equation was used to obtain the surface area (A_{BET}) and the Dubinin−Radushkevich equation was applied for the micropore volume calculation. The difference between the volume of N_2 adsorbed at 0.95 relative pressure and the micropore volume was taken as mesopore volume.

The amount of surface oxygen groups of the ACs was determined by temperature programmed desorption (TPD), heating 0.1 g of the AC sample up to 1100 °C in a vertical quartz tube under continuous N_2 flow of 1 $NL \cdot min^{-1}$ at a heating rate of 10 $°C \cdot min^{-1}$. The evolved amounts of CO and CO_2 were analyzed by means of a nondispersive infrared absorption analyzer (Siemens, model Ultramat 22). The CO and CO_2 TPD profiles were deconvoluted using PeakFit 4.12 software, selecting a multiple Gaussian function to fit each deconvolution peak of the TPD profile.[35] The characterization of fresh and heat-treated ACs is depicted in Table 1.

$OmimPF_6$ and phenol were used as adsorptive solutes and were not purified prior to use (purity of 99%). They were supplied by Iolitec and Sigma-Aldrich, respectively. Distilled water was employed for preparing all the solutions.

2.2. Batch Mode Adsorption Studies. The effect of adsorbent particle size (100−2000 μm), initial $OmimPF_6$ concentration (0.1−3.2 $mmol \cdot L^{-1}$), and temperature (308−348 K) on the adsorption kinetic and the equilibrium was studied with MkU in batch stirred tank runs. For the kinetic tests, 50 mL of $OmimPF_6$ aqueous solution of predetermined initial concentration was placed in stoppered flasks together with AC (1 $g \cdot L^{-1}$). The flasks were stirred at 200 rpm equivalent stirring rate in a thermostatted rotary shaker (Julabo Shake Temp, model SW-22) for contact times between 0 and 400 min. The equilibrium capacities for these experiments were obtained at an equilibration time of 5 days.

The study of the influence of stirring rate was carried out in a 1 L jacketed glass tank with mechanical stirring. 500 mL of 3.2 $mmol \cdot g^{-1}$ $OmimPF_6$ solution was placed into the tank with the AC (1 $g \cdot L^{-1}$) at 308 K. Samples (200 μL) were collected at regular contact times.

$OmimPF_6$ and phenol concentration in water was determined by UV spectroscopy (Varian, model Cary 1E) at 212 and 271 nm, respectively, which were the maximum of absorption spectra measured for these compounds.

For the sake of easier visualization of the experimental data trends, the kinetic curves were adjusted to a hyperbolic−type function ($q_t = (At)/(B + t)$, where and A and B are empirical coefficients, q_t, $mmol \cdot g^{-1}$, is the amount of adsorbate on the adsorbent at time t, min) and the resulting lines are represented in Figures 3−6.

2.3. Adsorption Kinetic Models. Table 1S in the Supporting Information summarizes the five kinetic models checked in this work to describe the adsorbate concentration onto the adsorbent (q_t, $mmol \cdot g^{-1}$) as a function of the contact time (t, min). The experimental q_t values were obtained as indicated using the MkU activated carbon as adsorbent. The hyperbolic model (2)[36] is a simple mathematical equation widely used to fit kinetic experimental data in terms of the empirical coefficients q_e ($mmol \cdot g^{-1}$) and k_f (min). The parameter q_e is the asymptotic value of q_t and is commonly used as a reference of maximum uptake of solute onto the adsorbent. The pseudo-first-order equation (3) for the liquid−solid adsorption is an empirical kinetic model proposed in the Lagergren's original paper,[37] which provides a pseudo-first-order rate constant k_1 (min^{-1}) by defining the driving force for the process as $(q_e - q_t)$. Pseudo-second-order (4) and Lagergren (5) models[38,39] are modifications of the pseudo-first-order equation by defining the driving adsorption forces as $(q_e - q_t)^2$ and $(q_e - q_t)^n$, respectively, providing the apparent rate constants k_2 and k_s ($g \cdot mol^{-1} \cdot min^{-1}$) for the adsorption process. In these last three simple models, all the steps of adsorption such as external diffusion, internal diffusion, and adsorption are lumped together in the corresponding rate constants and it is assumed that the difference between the

dx.doi.org/10.1021/ie3028729 | Ind. Eng. Chem. Res. 2013, 52, 2969−2976

Table 2. Physical Properties of $OmimPF_6$ and Phenol of Interest for Adsorption

	density ($g \cdot cm^{-3}$)[a]	viscosity ($mPa \cdot s^{-1}$)[a]	mol. vol. ($Å^3$)[a]	mol. wt ($g \cdot mol^{-1}$)	surface tension ($mN \cdot m^{-1}$)[a]	Log K_{ow}	parachor ($cm^3 \cdot mN^{1/4} \cdot mol^{-1} \cdot m^{-1/4}$)
$OmimPF_6$	1.19	85.7	457	340.3	34.9 [45]	3.9	694.2
phenol	1.07	10	121	94.1	39.3[b] [46]	1.4	220.2

[a]Density, viscosity, molecular volume, and Log K_{ow} obtained from COSMO-RS (computational details available in the Supporting Information). [b]T = 313 K.

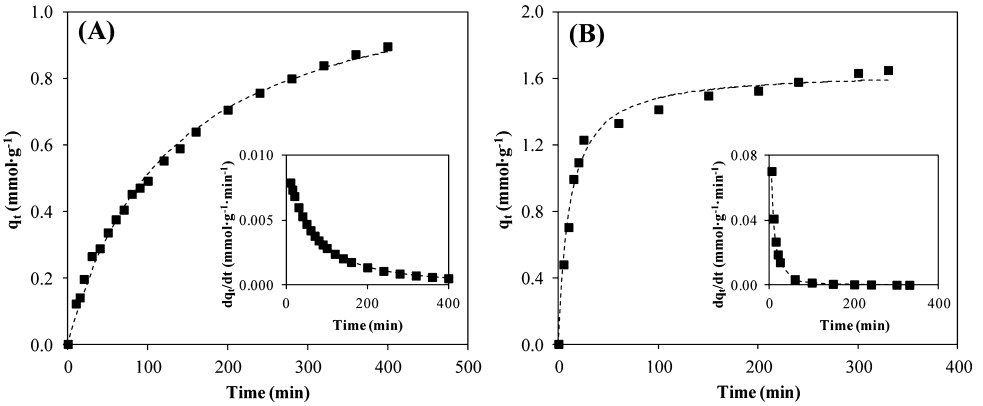

Figure 1. Experimental curves for the adsorption kinetics of $OmimPF_6$ (A) and phenol (B) onto MkU (d_p: 1000−2000 μm, 1000 mg·L^{-1} initial IL concentration, 200 rpm, 308 K).

average and the equilibrium solid phase concentrations is the driving force for adsorption. On the other hand, the intraparticle diffusion model[40] is a phenomenological kinetic model that assumes that adsorbate transport through the adsorbent particle is the prevailing rate-controlling step in the adsorption process, which is often the case, especially in well stirred batch systems.[30,41−43] The parameter k_{id} (μmol·g^{-1}·min$^{-0.5}$) is defined as the pore diffusion rate constant, whereas the intercept I is a constant related with the thickness of boundary layer.

3. RESULTS AND DISCUSSION

3.1. Comparison of the Adsorption Kinetics of $OmimPF_6$ and Phenol. Table 2 compares the physical properties of $OmimPF_6$ and phenol of interest for adsorption.[44,45] As can be seen, $OmimPF_6$ presents much higher viscosity and molecular volume than phenol. Looking at the values of Log K_{ow}, $OmimPF_6$ presents higher hydrophobicity than phenol and the parachor value suggests a higher trend of $OmimPF_6$ to be adsorbed onto AC. These characteristics anticipate lower rates of physical adsorption with ACs for $OmimPF_6$.

Figure 1 shows the adsorption kinetic curves of phenol (1A) and $OmimPF_6$ (1B) with commercial activated carbon MkU. In spite of the fact that equilibrium experiments revealed almost similar adsorption equilibrium capacity (1.32 and 1.68 mmol·g^{-1} for $OmimPF_6$ and phenol, respectively) of MkU for both solutes at equivalent aqueous phase concentration, important differences were found regarding the kinetic behavior of these solutes. Thus, while an uptake of 1 mmol·g^{-1} of phenol was achieved at 10 min, to obtain equivalent adsorption of $OmimPF_6$ took around 600 min. Therefore, the adsorption rate of a common IL, such as $OmimPF_6$, onto AC seems to be significantly lower than that of conventional low molecular weight organic solutes, which can be due to its higher molecular volume, viscosity, and density, giving rise to a lower pore diffusivity. Thus, the following will be focused on analyzing the effects of operating conditions on the rate of IL adsorption by ACs.

Figure 1 shows the kinetic curves obtained for the adsorption of $OmimPF_6$ and phenol, with the activated carbon MkU. Table S2 of the Supporting Information summarizes the values of the fitting parameters for the five kinetic models checked. Reasonably to frankly good correlation coefficients (R^2) were obtained for all the kinetic models evaluated. All of them serve to describe fairly well the experimental data (see Figure S1 in the Supporting Information). The models fulfill the statistical criteria since the confidence interval for their parameters does not include the zero value. Statistical analysis shows that Lagergren model provides the best description of kinetic curves for $OmimPF_6$ solute, with an R^2 value of 0.997 and by far the lowest value of mean standard deviation (RMSD = 0.6%). Remarkably, the apparent kinetic constant (k_s) obtained by Lagergren model indicates 6-fold lower adsorption rates for IL adsorption than for phenol. Although these four empirical simple kinetic models satisfactorily reproduced the experimental data of Figure 1, they do not provide mechanistic information on the adsorption process. Typically, various phenomena can control the adsorption rate, the most limiting being related with diffusion, including external, boundary layer, and intraparticle diffusion. A phenomenological intraparticle diffusion model (eq 6 in Table S1 of the Supporting Information) was also checked to analyze the measured kinetic behavior of IL adsorption onto AC. Figure 2 depicts the experimental and calculated values of q_t vs $t^{1/2}$ for IL and phenol adsorption (see the fitting values of k_{id} and I together with the statistical parameters in Table S2 of the Supporting Information). As can be seen, the adsorption curve for phenol shows two regions, being the first linear part ($0 < t < 25$ min) attributed to intraparticle diffusion and the second plateau-like branch to the equilibrium-approaching stage. In contrast, $OmimPF_6$ presents a wider time range for the linear part ($0 < t < 225$ min). These results, together with the negligible I value (0.01), the high correlation coefficient (R^2 = 0.996) and

dx.doi.org/10.1021/ie3028729 | Ind. Eng. Chem. Res. 2013, 52, 2969−2976

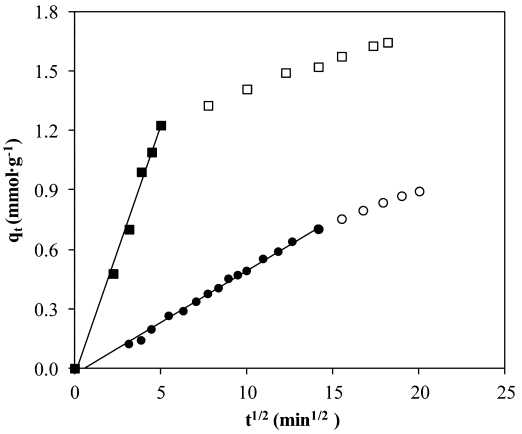

Figure 2. Fitting of the intraparticle diffusion model for the adsorption of phenol (■, □) and $OmimPF_6$ (●, ○) onto MkU (d_p: 1000−2000 μm, 1000 mg·L^{-1}, 200 rpm, 308 K).

the low SD (0.02) and RMSD (6.6%) values, indicate that intraparticle diffusion may be the rate-controlling step during the first stage of adsorption of the hydrophobic IL $OmimPF_6$ onto MkU, which is a common situation in the adsorption of organic compounds by ACs.[46,47]

3.2. Effect of Operating Conditions on the Kinetics of $OmimPF_6$ Adsorption. In this work, the effect of the main operating conditions (stirring velocity, AC particle size, temperature, and initial concentration of IL) on the adsorption rate of hydrophobic IL ($OmimPF_6$) onto commercial activated carbon MkU were investigated. It was found that the intraparticle diffusion model (eq 6 in Table 1 of the Supporting Information) enables a satisfactory reproduction of the experimental adsorption curves of $OmimPF_6$ onto MkU for the different operating conditions tested, considering the linear region of the corresponding experimental curves (see the values of the statistical parameters R^2, SD, and RMSD for the intraparticle diffusion model in Table S3, which were obtained from the kinetic data shown in Figure S2 of the Supporting Information).

The effect of stirring velocity was tested within the range 300−700 rpm using the commercial MkU with 500−1000 μm particle size, at 3.2 mmol·L^{-1} (1000 mg·L^{-1}) of IL initial concentration and 308 K. No significant differences were observed (see Table S3 and Figure S3 in the Supporting Information), indicating that external mass transfer does not have a significant influence on the adsorption kinetics of $OmimPF_6$ under the operating conditions used. The adsorption capacity at equilibrium at these operating conditions was around 1.3 mmol·g^{-1}.

Figure 3 shows the results obtained at different particle sizes of MkU. As can be seen, the adsorption rate of $OmimPF_6$ clearly increases when decreasing the AC particle size, whereas the equilibrium capacity remains almost constant. The intraparticle diffusion model provides an adequate description of these experimental results (see the low I, SD, and RMSD and the good R^2 values summarized in Table S3 of the Supporting Information). The values obtained for the pore diffusion rate constant (k_{id}) shifted from 52.4 μmol·g^{-1}·min$^{-0.5}$ for d_p = 2000−1000 to 280.6 μmol·g^{-1}·min$^{-0.5}$ for d_p = 300−100 μm particle size (Figure 3). These results strongly support the conclusion that intraparticle diffusion is the step controlling the rate of adsorption of $OmimPF_6$ onto AC, as it occurs in general with organic solutes, most in particular, those of high molecular size.[48,49] The effect of particle size on the adsorption kinetics was much lower in the case of phenol (see Figure S4 in the Supporting Information).

The influence of the initial IL concentration (0.1−3.2 mmol·L^{-1}) on the adsorption onto MkU is shown in Figure 4 and summarized in Table S3 of the Supporting Information. Previous physicochemical,[50,51] spectroscopic,[52] and computational[53] studies on imidazolium-based ILs with PF_6^- anion indicated the absence of self-aggregated IL species in water solution at the concentration range used in this work. The shape of the adsorption isotherms for $OmimPF_6$ onto commercial MkU activated carbon at different temperatures supports this conclusion.[23,24]

As can be seen, the values of k_{id} increase substantially with the particle size. Increasing the initial concentration provokes a higher driving force giving rise to a faster adsorption in agreement with the commonly observed with conventional organic solutes.[54,55] Thanks to this higher driving force, the plateau of the kinetic curves is reached at nearly similar contact time (~200 min), in spite of the fact that a significantly higher amount of IL is adsorbed onto the AC at equilibrium (q_s) as the initial concentration increases within the range tested (q_s varies from 0.68 to 1.32 mmol·g^{-1}).

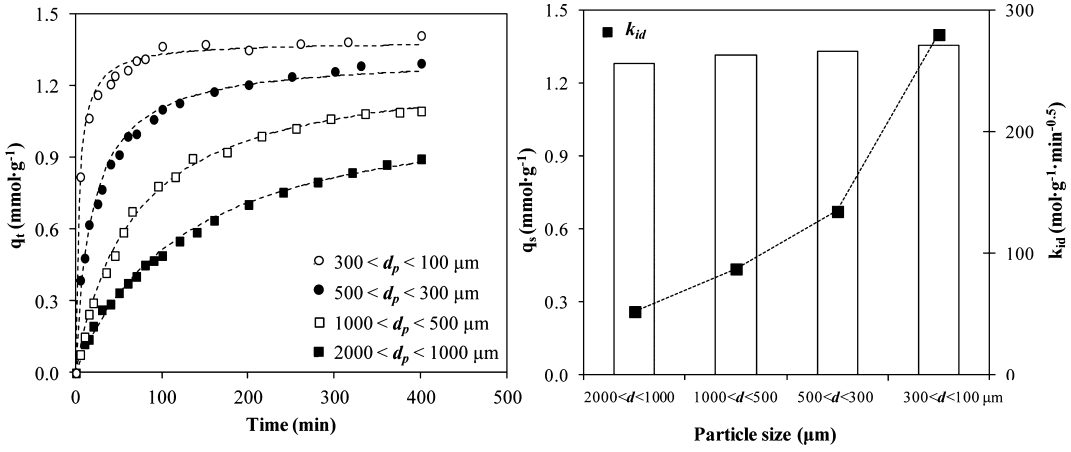

Figure 3. Effect of the particle size on the kinetics of adsorption of $OmimPF_6$ onto MkU at different particle size (200 rpm; 3.2 mmol·L^{-1} initial IL concentration; 308 K).

dx.doi.org/10.1021/ie3028729 | Ind. Eng. Chem. Res. 2013, 52, 2969−2976

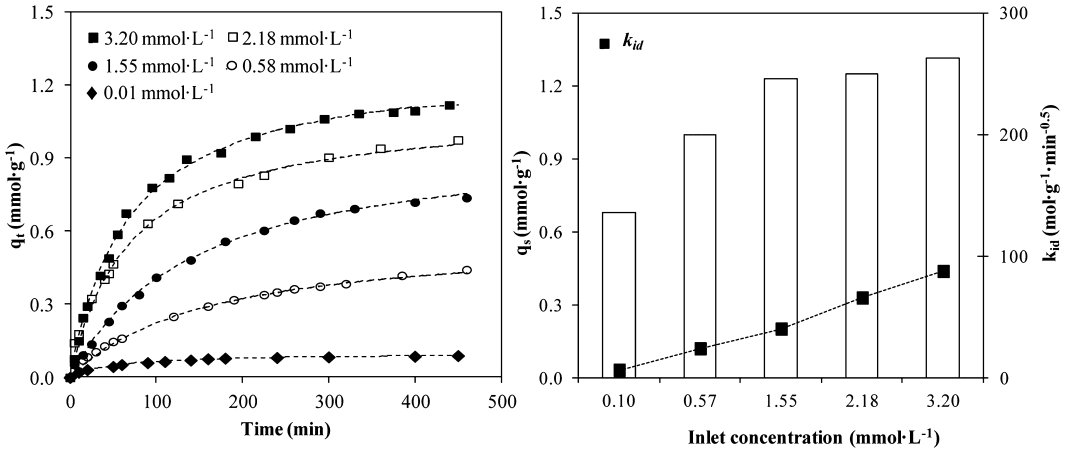

Figure 4. Effect of the initial concentration of $OmimPF_6$ on the kinetics of adsorption onto MkU (200 rpm, d_p = 500−1000 μm, 308 K).

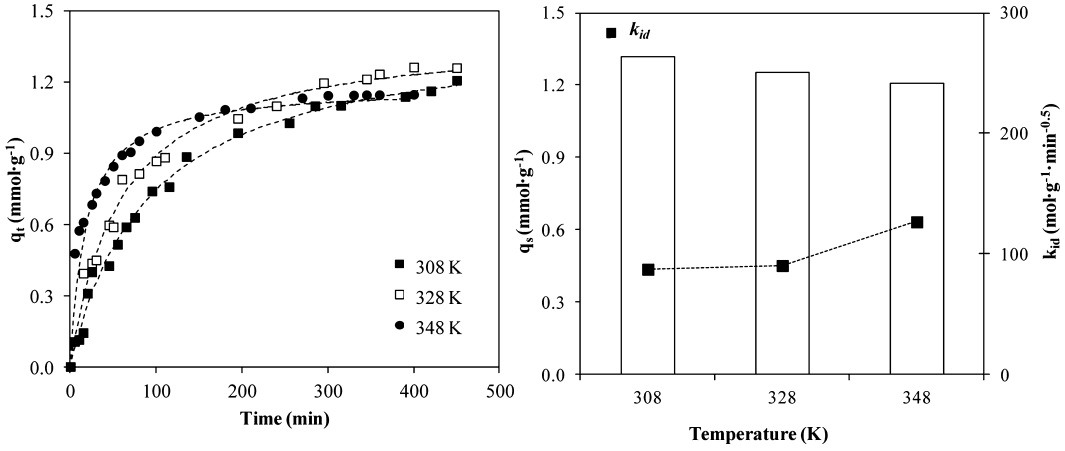

Figure 5. Effect of temperature on the adsorption of $OmimPF_6$ onto MkU (200 rpm; d_p = 500−1000 μm; 3.2 mmol·L^{-1} initial concentration).

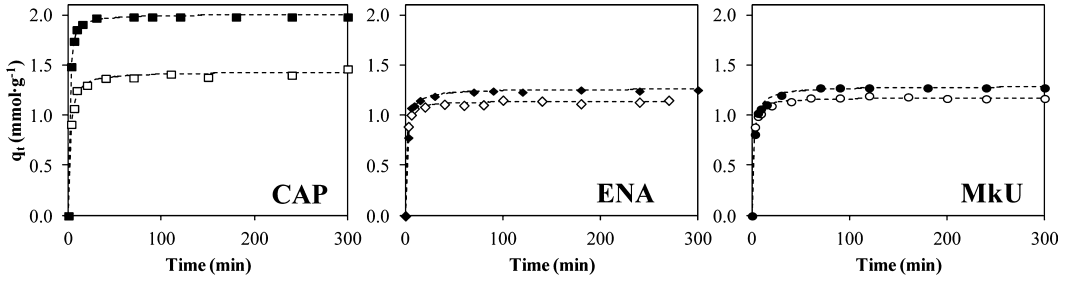

Figure 6. Experimental curves for the adsorption kinetics of $OmimPF_6$ onto the fresh (solid symbols) and heat-treated (open symbols) activated carbons (d_p < 100 μm; 1.6 mmol·L^{-1} initial concentration; 200 rpm; 308 K).

Figure 5 shows the effect of temperature on the adsorption of $OmimPF_6$ on MkU within the range of 308−348 K. The values of adsorption rate constant, k_{id}, obtained from the intraparticle diffusion model increased with temperature from 88 μmol·g^{-1}·$min^{-0.5}$ (308 K) to 120 μmol·g^{-1}·$min^{-0.5}$ (348 K), (Table S3 of Supporting Information). On the other hand, the equilibrium capacity (q_s) is higher at lower temperature, as expected in physical adsorption.[56−58]

From a technical point of view, in spite of the lower equilibrium capacity, working at higher temperature has the advantage of a faster adsorption. Thus, q_t values ca. 1 mmol·g^{-1} are reached in around 150 min at 348 K, whereas contact times higher than 300 min are needed to achieve such capacity at 308 K. For long contact times, a higher capacity is obtained at lower temperature, but this would not be justified by the high contact time that would be required. The apparent activation energy for the adsorption of $OmimPF_6$ onto MkU can be estimated assuming an Arrhenius type dependence of the intraparticle diffusion rate constant with temperature. A value of 8.8 kJ·mol^{-1} was obtained, consistent with a mechanism of physical adsorption controlled by intraparticle diffusion.[47,58,59]

3.3. Adsorption of $OmimPF_6$ onto Modified Activated Carbons. A recent study by our group[24] showed that the uptake of hydrophobic ILs from water by adsorption can be increased by selecting ACs with (i) high surface area, (ii) high content of accessible pores narrower than 8 nm, and (iii) low concentration of oxygen surface groups on the carbon surface. In the current work, the effect of the adsorbent characteristics

dx.doi.org/10.1021/ie3028729 | Ind. Eng. Chem. Res. 2013, 52, 2969−2976

on the kinetics of adsorption of $OmimPF_6$ from aqueous phase has been analyzed. For this purpose, three commercial ACs (MkU, CAP, and ENA) were subjected to thermal treatment in order to reduce their oxygenated surface groups content, giving rise to MkU-900, CAP-900, and ENA-900. The set of ACs prepared were compared at equivalent small particle sizes (d_p < 100 μm). The characterization of the fresh and heat-treated ACs is summarized in Table 1. The 77 K N_2 adsorption−desorption isotherms (included as Supporting Information, Figure S5) showed that the thermal treatment does not affect significantly the porous structure of MkU and ENA, whereas it has a much more marked effect in the case of CAP. As expected, the results from deconvolution of the TPD curves (Figure S6 of the Supporting Information) showed a significant decrease in the amount of surface oxygen groups of the heat-treated carbons (see Table 1).[60] This thermal treatment is effective to reduce the concentration of surface oxygen groups from the AC,[61] as it is collected in Table 1.

Figure 6 shows the experimental kinetic curves for the adsorption of $OmimPF_6$ onto the fresh and modified ACs with small particle size (d_p < 100 μm). These results were well described by the intraparticle diffusion model (see R^2, SD, and RMSD in Table S4, Supporting Information). High values of the pore diffusion rate constant (k_{id} > 350 μmol·g^{-1}·min$^{-0.5}$) were obtained in all cases. The fresh MkU and ENA gave quite similar k_{id} values, and their thermal treatment had only a small effect on the adsorption rate of $OmimPF_6$. On the opposite, frankly important differences were observed in the case of CAP where the adsorption rate constant decreased by 35% upon thermal treatment. In addition to this, the high value of the I parameter may suggest that intraparticle diffusion is not the rate-controlling step for the fresh CAP, probably due to its high external area. CAP-900 shows a much lower external area and a lower value of the I parameter. On the other hand, the equilibrium capacity (q_s) for the adsorption of the hydrophobic IL $OmimPF_6$ onto ACs is mainly determined by the surface area and the volume of pore <8 nm of the adsorbent;[25] as a consequence, the q_s value decreases in all cases upon thermal treatment of the ACs, being that effect much more accused in the case of CAP according to the remarkably decrease of A_{BET} and $V_{microp.}$ for the treated CAP-900 sample.

4. CONCLUSIONS

A detailed kinetic study on the adsorption of the hydrophobic ionic liquid 1-methyl-3-octilimidazolium hexafluorophosphate ($OmimPF_6$) onto three commercial and modified activated carbons from water solution has been carried out, including the analysis of the influence of main operating conditions as stirring velocity, adsorbent particle size, temperature, and solute initial concentration. The results showed relatively slow adsorption of $OmimPF_6$ with respect to a benchmark organic solute as phenol. Different kinetic models have been tested to describe the measured curves of IL onto AC. Experimental and theoretical evidence indicated that intraparticle diffusion is the prevailing rate-controlling step in the adsorption mechanism of the $OmimPF_6$ onto AC. As a result, it is obtained for a variety of ACs with different porous structure and chemical surface that the adsorption rate of the IL can be efficiently enhanced by decreasing the adsorbent particle size. The new insights on the knowledge of IL adsorption by ACs indicated the viability of this treatment at larger scale for removal/recovery of IL from industrial wastewaters.

■ ASSOCIATED CONTENT

Supporting Information

Experimental versus predicted curves for the adsorption kinetics of $OmimPF_6$ and phenol onto MkU (Figure S1). Fitting of the intraparticle diffusion model for adsorption of $OmimPF_6$ onto MkU at different operating conditions (Figure S2). Effect of stirring velocity on the adsorption kinetics of $OmimPF_6$ onto MkU (Figure S3). Experimental curves for adsorption kinetics of phenol onto MkU at different particle sizes and 308 K (Figure S4). N_2 adsorption/desorption isotherms at 77 K of fresh and heat-treated ACs (Figure S5). TPD spectra of fresh and heat-treated (Figure S6). Kinetic models checked (Table S1). Thermodynamic and kinetic analysis for the adsorption of $OmimPF_6$ and phenol onto MkU (Table S2). Equilibrium capacity and kinetic analysis for the adsorption of $OmimPF_6$ onto commercial MkU at different operating conditions (Table S3). Equilibrium capacity and kinetic analysis for the adsorption of $OmimPF_6$ onto fresh and heat-treated activated carbons (Table S4). This material is available free of charge via the Internet at http://pubs.acs.org.

■ AUTHOR INFORMATION

Corresponding Author

*Telephone: 34 91 497 35 98. Fax: 34 91 497 35 16. E-mail: jesus.lemus@uam.es.

Notes

The authors declare no competing financial interest.

■ ACKNOWLEDGMENTS

The authors are grateful to the Spanish "Ministerio de Ciencia e Innovación (MICINN)" and "Comunidad de Madrid" for financial support (Project Nos. CTQ2011-26758, CTQ2009-09983, and S2009/PPQ-1545).

■ REFERENCES

(1) Plechkova, N. V.; Seddon, K. R. Applications of Ionic Liquids in the Chemical Industry. *Chem. Soc. Rev.* **2008**, *1*, 123.

(2) Wasserscheid, P.; Welton, T. *Ionic Liquids in Synthesis*; Wiley-VCH: Weinheim, 2008.

(3) Ranke, J.; Stolte, S.; Stormann, R.; Arning, J.; Jastorff, B. Design of Sustainable Chemical Products—The Example of Ionic Liquids. *Chem. Rev.* **2007**, *6*, 2183.

(4) Kokorin, A. *Ionic Liquids: Theory, Properties, New Approaches*; Rijeka, Croatia, 2011.

(5) Brennecke, J. F.; Maginn, E. J. Ionic liquids: Innovative Fluids for Chemical Processing. *AIChE J.* **2001**, *11*, 2384−2389.

(6) Huang, J.; Riisager, A.; Berg, R. W.; Fehrmann, R. Tuning Ionic Liquids for High Gas Solubility and Reversible Gas Sorption. *J. Mol. Catal. A: Chem.* **2008**, *2*, 170−176.

(7) Gardas, R. L.; Coutinho, J. A. P. A Group Contribution Method for Viscosity Estimation of Ionic Liquids. *Fluid Phase Equilib.* **2008**, *1*−*2*, 195.

(8) Fernandez, J. F.; Neumann, J.; Thoeming, J. Regeneration, Recovery and Removal of Ionic Liquids. *Curr. Org. Chem.* **2011**, *12*, 1992.

(9) Petkovic, M.; Seddon, K.; Rebelo, L.; Pereira, C. Ionic liquids: a Pathway to Environmental Acceptability. *Chem. Soc. Rev.* **2011**, *3*, 1383.

(10) Zhao, D. B.; Liao, Y. C.; Zhang, Z. D. Toxicity of ionic liquids, Clean-Soil Air Water. *Clean: Soil, Air, Water* **2007**, *1*, 42.

(11) Torrecilla, J. S.; Palomar, J.; Lemus, J.; Rodriguez, F. A Quantum-Chemical-Based Guide to Analyze/Quantify the Cytotoxicity of Ionic Liquids. *Green Chem.* **2010**, *1*, 123−134.

(12) Coleman, D.; Gathergood, N. Biodegradation Studies of Ionic Liquids. *Chem. Soc. Rev.* **2010**, *2*, 600.

(13) Stepnowski, P.; Zaleska, A. Comparison of Different Advanced Oxidation Processes for the Degradation of Room Temperature Ionic Liquids. *J. Photochem. Photobiol., A* **2005**, *1*, 45.
(14) Czerwicka, M.; Stolte, S.; Muller, A.; Siedlecka, E.; Golebiowski, M.; Kumirska, J. Identification of Ionic Liquid Breakdown Products in an Advanced Oxidation System. *J. Hazard. Mater.* **2009**, *1*−*3*, 478.
(15) Stolte, S.; Arning, J.; Thoeming, J. Biodegradability of Ionic Liquids—Test Procedures and Structural Design. *Chem. Eng. Technol.* **2011**, *9*, 1454.
(16) Abrusci, C.; Palomar, J.; Pablos, J.; Rodriguez, F.; Catalina, F. Efficient Biodegradation of Common Ionic Liquids by *Sphingomonas paucimobilis* Bacterium. *Green Chem.* **2011**, *3*, 709.
(17) Meindersma, G. W. de Haan, A. B. Conceptual Process Design for Aromatic/Aliphatic Separation with Ionic Liquids. *Chem. Eng. Res. Des.* **2008**, *7A*, 745.
(18) Nockemann, P.; Binnemans, K.; Driesen, K. Purification of imidazolium ionic liquids for spectroscopic applications. *Chem. Phys. Lett.* **2005**, *1*−*3*, 131.
(19) Krockel, J.; Kragl, U. Nanofiltration for the Separation of Nonvolatile Products from Solutions Containing Ionic Liquids. *Chem. Eng. Technol.* **2003**, *11*, 1166.
(20) Schafer, T.; Rodrigues, C. M.; Afonso, C. A. M.; Crespo, J. G. Selective Recovery of Solutes from Ionic Liquids by Pervaporation—A Novel Approach for Purification and Green Processing. *Chem. Commun.* **2001**, *17*, 1622.
(21) Mahmoud, M.; Al Bishri, H. Supported Hydrophobic Ionic Liquid on Nano-Silica for Adsorption of Lead. *Chem. Eng. J.* **2011**, *1*, 157.
(22) Anthony, J. L.; Maginn, E. J.; Brennecke, J. F. Solution Thermodynamics of Imidazolium-Based Ionic Liquids and Water. *J. Phys. Chem. B* **2001**, *44*, 10942.
(23) Palomar, J.; Lemus, J.; Gilarranz, M. A.; Rodriguez, J. J. Adsorption of Ionic Liquids from aqueous Effluents by Activated Carbon. *Carbon* **2009**, *7*, 1846.
(24) Lemus, J.; Palomar, J.; Heras, F.; Gilarranz, M. A.; Rodriguez, J. J. Developing Criteria for the Recovery of Ionic Liquids from Aqueous Phase by Adsorption with Activated Carbon. *Sep. Purif. Technol.* **2012**, 11.
(25) Farooq, A.; Reinert, L.; Levêque, J.; Papaiconomou, N.; Irfan, N.; Duclaux, L. Adsorption of Ionic Liquids onto Activated Carbons: Effect of pH and Temperature. *Microporous Mesoporous Mater.* **2012**, *0*, 55.
(26) Lemus, J.; Palomar, J.; Gilarranz, M. A.; Rodriguez, J. J. Characterization of Supported Ionic Liquid Phase (SILP) Materials Prepared from Different Supports. *Adsorption* **2011**, *3*, 561.
(27) Bansal, R.; Goyal, M. *Activated Carbon Adsorption*; Taylor and Francis: Boca Raton, FL, 2005.
(28) Yin, C. Y.; Aroua, M. K.; Daud, W. M. A. W. Review of Modifications of Activated Carbon for Enhancing Contaminant Uptakes from Aqueous Solutions. *Sep. Purif. Technol.* **2007**, 3, 403.
(29) Rouquerol, J.; Rouquerol, F.; Sing, K. Adsorption by Powders and Porous Solids. *Principles, Methodology, and Applications*; Academic Press: London, 1999.
(30) Kannan, N.; Sundaram, M. Kinetics and Mechanism of Removal of Methylene Blue by Adsorption on Various Carbons—A Comparative Study. *Dyes Pigm.* **2001**, *1*, 25.
(31) Cotoruelo, L. M.; Marques, M. D.; Diaz, F. J.; Rodriguez-Mirasol, J.; Rodriguez, J. J.; Cordero, T. Equilibrium and Kinetic Study of Congo Red Adsorption onto Lignin-Based Activated Carbons. *Transp. Porous Media* **2010**, *3*, 573.
(32) McKay, G.; Blair, H.; Gardner, J. Adsorption of Dyes on Chitin 0.1. Equilibrium Studies. *J. Appl. Polym. Sci.* **1982**, *8*, 3043.
(33) Tsukamoto, M. Intraparticle Diffusion of Cesium and Strontium Cations into Rock Materials. *Chem. Geol.* **1991**, *1*, 31.
(34) Crank, J. *Mathematics of Diffusion*; Oxford at the Clarendon Press: London, 1956.
(35) Rey, A.; Faraldos, M.; Casas, J. A.; Zazo, J. A.; Bahamonde, A.; Rodriguez, J. J. Catalytic Wet Peroxide Oxidation of Phenol over Fe/AC Catalysts: Influence of Iron Precursor and Activated Carbon Surface. *Appl. Catal., A* **2009**, *1*−*2*, 69.
(36) Cotoruelo, L. M.; Marques, M. D.; Rodriguez-Mirasol, J.; Rodriguez, J. J.; Cordero, T. Cationic Dyes Removal by Multilayer Adsorption on Activated Carbons from Lignin. *J. Porous Mater.* **2011**, *6*, 693.
(37) Ho, Y. Citation Review of Lagergren Kinetic Rate Equation on Adsorption Reactions. *Scientometrics* **2004**, *1*, 171.
(38) Ho, Y. S.; McKay, G. Pseudo-Second Order Model for Sorption Processes. *Process Biochem.* **1999**, *5*, 451.
(39) Cotoruelo, L. M.; Marques, M. D.; Rodriguez-Mirasol, J.; Rodriguez, J. J.; Cordero, T. Lignin-Based Activated Carbons for Adsorption of Sodium Dodecylbenzene Sulfonate: Equilibrium and Kinetic Studies. *J. Colloid Interface Sci.* **2009**, *1*, 39.
(40) Srivastava, S.; Tyagi, R.; Pant, N. Adsorption of Heavy-Metal Ions on Carbonaceous Material Developed from the Waste Slurry Generated in Local Fertilizer Plants. *Water Res.* **1989**, *9*, 1161.
(41) Mezenner, N. Y.; Bensmaili, A. Kinetics and Thermodynamic Study of Phosphate Adsorption on Iron Hydroxide-Eggshell Waste. *Chem. Eng. J.* **2009**, *2*−*3*, 87−96.
(42) Qadeer, R. Kinetic Study of Erbium Ion Adsorption on Activated Charcoal from Aqueous Solutions. *Adsorption* **2005**, *1*, 51.
(43) Qiu, H.; Lv, L.; Pan, B.; Zhang, Q.; Zhang, W.; Zhang, Q. Critical Review in Adsorption Kinetic Models. *J. Zhejiang Univ., Sci., A.* **2009**, *5*, 716.
(44) Gardas, R. L.; Coutinho, J. A. P. Applying a QSPR Correlation to the Prediction of Surface Tensions of Ionic Liquids. *Fluid Phase Equilib.* **2008**, *1*−*2*, 57.
(45) Poling, B.; Prausnitz, J.; O'Connell, J. *The Properties of Gases and Liquids*, 5th ed.; McGraw-Hill: New York, 1958.
(46) Moreno-Castilla, C. Adsorption of Organic Molecules from Aqueous Solutions on Carbon Materials. *Carbon* **2004**, *1*, 83.
(47) Sarkar, M.; Acharya, P. K.; Bhattacharya, B. Modeling the Adsorption Kinetics of some Priority Organic Pollutants in Water from Diffusion and Activation Energy parameters. *J. Colloid Interface Sci.* **2003**, *1*, 28.
(48) Vadivelan, V.; Kumar, K. Equilibrium, Kinetics, Mechanism, and Process Design for the Sorption of Methylene Blue onto Rice Husk. *J. Colloid Interface Sci.* **2005**, *1*, 90.
(49) Porkodi, K.; Kumar, K. V. Equilibrium, Kinetics and Mechanism Modeling and Simulation of Basic and Acid Dyes Sorption onto Jute Fiber Carbon: Eosin Yellow, Malachite Green, and Crystal Violet Single Component Systems. *J. Hazard. Mater.* **2007**, *1*−*2*, 311.
(50) Blesic, M.; Marques, M. H.; Plechkova, N. V.; Seddon, K. R.; Rebelo, L. P. N.; Lopes, A. Self-Aggregation of Ionic Liquids: Micelle Formation in Aqueous Solution. *Green Chem.* **2007**, *5*, 481.
(51) Modaressi, A.; Sifaoui, H.; Mielcarz, M.; Domanska, U.; Rogalski, M. Influence of the Molecular Structure on the Aggregation of Imidazolium Ionic Liquids in Aqueous Solutions. *Colloids Surf., A* **2007**, 1−3.
(52) Katsuta, S.; Yamaguchi, N.; Ogawa, R.; Kudo, Y.; Takeda, Y. Distribution of 1-Alkyl-3-methylimidazolium Ions and Their Ion Pairs between Dichloromethane and Water. *Anal. Sci.* **2008**, *10*, 1261.
(53) Palomar, J.; Ferro, V. R.; Gilarranz, M. A.; Rodriguez, J. J. Computational Approach to Nuclear Magnetic Resonance in 1-Alkyl-3-methylimidazolium Ionic Liquids. *J. Phys. Chem. B* **2007**, *1*, 168.
(54) Navarrete-Casas, R.; Navarrete-Guijosa, A.; Valenzuela-Calahorro, C.; Lopez-Gonzalez, J. D.; Garcia-Rodriguez, A. Study of Lithium Ion Exchange by Two Synthetic Zeolites: Kinetics and Equilibrium. *J. Colloid Interface Sci.* **2007**, *2*, 345.
(55) Li, L.; Liu, S.; Zhu, T. Application of Activated Carbon Derived from Scrap Tires for Adsorption of Rhodamine. *J. Environ. Sci.* **2010**, *8*, 1273.
(56) Demirbas, E.; Nas, M. Z. Batch Kinetic and Equilibrium Studies of Adsorption of Reactive Blue 21 by Fly Ash and Sepiolite. *Desalination* **2009**, *1*−*3*, 8.
(57) Demirbas, E.; Dizge, N.; Sulak, M. T.; Kobya, M. Adsorption Kinetics and Equilibrium of Copper from Aqueous Solutions Using Hazelnut Shell Activated Carbon. *Chem. Eng. J.* **2009**, *2*−*3*, 480.

(58) Acemioglu, B. Batch Kinetic Study of Sorption of Methylene Blue by Perlite. *Chem. Eng. J.* **2005**, *1*, 73.
(59) Dogan, M.; Ozdemir, Y.; Alkan, M. Adsorption Kinetics and Mechanism of Cationic Methyl Violet and Methylene Blue Dyes onto Sepiolite. *Dyes Pigm.* **2007**, *3*, 701.
(60) Figueiredo, J. L.; Pereira, M. F. R. The Role of Surface Chemistry in Catalysis with Carbons. *Catal. Today* **2010**, *150*, 2.
(61) Menéndez, J. A.; Phillips, J.; Xia, B.; Radovic, L. R. On the Modification and Characterization of Chemical Surface Properties of Activated Carbon: In the Search of Carbons with Stable Basic Properties. *Langmuir* **1996**, *12* (18), 4404.